Stress-Strain and Deformation Characteristics of an Unsaturated Soil-Cement Interface under Different Overburden Stresses and Grouting Pressures

M. A. Hossain[1] and J. H. Yin[2]
[1]*Department of Civil Engineering, Rajshahi University of Engineering & Technology, Rajshahi, Bangladesh*
[2]*Department of Civil and Environmental Engineering, The Hong Kong Polytechnic University, Hong Kong, China*
E-mail: akhtar412002@yahoo.com

ABSTRACT: The most important parameters, by which the shear strength of any interface may be affected, are overburden stress and degree of saturation. Nowadays, grouting pressure is considered as another important parameter, which affects the interface behavior. In addition to gravity grouting, pressure grouting has been widely used to grout insitu soil-cement grout interfaces, like interfaces of soil-nail, soil-pile, and soil-anchor. In the present study, a series of interface direct shear tests were performed between a compacted completely decomposed granite (CDG) soil and cement grout under different overburden stresses, matric suctions, and grouting pressures. The stress-strain and deformation characteristics of the pressure grouted interface are similar to that of the CDG soil. However, the dilation values of soil-cement interface under different grouting pressures are smaller compared to CDG soil. The interface shear strength envelopes are approximately linear, and the apparent interface friction angle and adhesion intercept increase with matric suction for particular grouting pressures. On the contrary, the apparent interface friction angle decreases with pressure grouting for different matric suctions except saturated condition at which it remains constant.

KEYWORDS: CDG soil, Direct shear, Matric suction, Grouting pressure, Overburden stress, Cement grout, Interface.

1. INTRODUCTION

Soil-nails have been used extensively all over the world to stabilize the substandard soil slopes. The ultimate shear strength at the interface between the structural surface and the surrounding soil surface is an important issue for the design and safety assessment of soil- nails. Overburden stress condition, type of grouting, degree of saturation of soil, and soil-nail surface roughness are the influential parameters, which affect the interface strength of soil-nail. The interface strength of soil-nails is determined by performing either field pullout tests (Heymann, 1993; Berglund and Oden, 1996; Pun and Shiu, 2007) or laboratory pullout tests (Franzen, 1998; Lee *et al.*, 2001; Chu and Yin, 2005; Yin and Zhou, 2009). Under the identical conditions, it is observed that the interface behavior of soil-nail pullout test is different from the soil-cement grout interface direct shear test (Chu and Yin, 2005). This may be attributed to limitations to control some boundary conditions in soil-nail pullout tests like stress acting on the surrounding of the nail surface is difficult to measure, less control of saturation, no uniform stress-strain rate, and deformation parameters cannot be obtained precisely. To overcome these limitations, direct shear tests can be used to determine the actual soil-cement grout interface behavior.

It is recognized that grouting pressure has an influence on the cast-insitu interface behavior. Yeung et al. (2005) performed field pullout tests on glass fiber reinforced polymer pipe nail in a CDG soil slope in Hong Kong. The test results showed that the pullout resistance significantly increases due to pressure grouting. Yin et al. (2008) presented a small number of laboratory pullout tests and discussed the influence of grouting pressure on the soil-nail pullout resistance. The test results stated that soil-nail pullout resistance increases with grouting pressure. Yin and Zhou (2009) conducted a series of laboratory soil-nail pullout tests under a combination of different grouting pressures and overburden stresses at nearly saturated condition. The test results showed that grouting pressure and overburden stress have interactional influence on the soil-nail pullout resistance. Hossain and Yin (2014) investigated the interface behavior between CDG soil and cement grout at saturated condition with different grouting pressures using a direct-shear apparatus with a special setup for interface testing. The test results indicated that the interface strength increases with grouting pressure.

Matric suction has a significant influence on the engineering behavior of unsaturated soil (Fredlund and Rahardjo, 1993; Burland and Ridley, 1996; Hossain and Yin, 2010a, b). Soil slopes are mainly unsaturated as the water table lies at a greater depth, and the water content of slopes increases due to infiltration of rain water during heavy raining. That is why, it is very important to determine the interface shear strength between grouted part of soil-nail and surrounding soil at both saturated and unsaturated conditions for the design and safety of the soil-nails. However, there is a lack of literature concerning the behavior of soil-cement interface at unsaturated condition.

Miller and Hamid (2007) performed interface tests between unsaturated Minco silt and stainless steel. The test results showed that the interface shear strength increases with the increase of net normal stress and matric suction. The failure envelope and suction envelope were quite linear. However, the shear strength of the soil was greater than the rough interface for similar stress conditions. Sharma et al. (2007) conducted soil-geomembrane interface laboratory tests with provision for the measurement of pore pressures close to the soil-geomembrane interface during shearing process. The test results suggested that soil suction contributes to shearing resistance at lower normal stress values. At higher normal stress values, the interface shear behavior appeared to be governed only by the magnitude of total normal stress. Hamid and Miller (2009) examined the interface behavior between unsaturated Minco silt and steel (smooth and rough surfaces). The test results indicated that matric suction contributes to the peak shear strength of unsaturated interfaces, and post-peak shear strength does not vary with changes in matric suction. Net normal stress affects both peak and post-peak shear strength, and the suction envelope for interface is nonlinear. Hossain and Yin (2012) described the interface behavior between compacted completely decomposed granite (CDG) soil and cement grout under different matric suctions with a net normal stress of 100 kPa. The test results reflected that the interface strength increases at lower matric suction, but decreases at higher suctions for that particular net stress.

This paper focuses on the interface behavior between compacted completely decomposed granite (CDG) soil and cement grout under different matric suctions (0, 50, 100, 200 and 300 kPa), overburden stresses (50, 100 and 300 kPa), and grouting pressures (0, 80, 130 and 250 kPa). A modified direct shear apparatus with a large shear box of 100.07 mm by 100.07 mm square with a special setup for interface testing is used to conduct the interface testing program.

2. INTERFACE SHEAR STRENGTH

2.1 Saturated Condition

Mohr-Coulomb failure criteria govern the interface shear strength for saturated case (0 kPa matric suction). Potyondy (1961) modified the Mohr-Coulomb's equation as follows with introducing the coefficient f_a for the reduction of cohesion, and a coefficient f_ϕ for the reduction of the internal soil friction angle in the interface model:

$$\tau_f = f_a c' + \sigma'_{nf} \tan(f_\phi \phi') \quad (1)$$

where, τ_f is the interface shear strength at failure; $f_a = \frac{c'_a}{c'}$; $f_\phi = \frac{\delta'}{\phi'}$; σ'_{nf} is the effective normal stress on the interface at failure; c'_a is the effective soil adhesion on the interface; δ' is the effective interface friction angle; c' is the effective cohesion of soil; and ϕ' is the effective angle of internal friction of soil. However, Kulhawy and Peterson (1979) found that adhesion or interface friction angle for different interfaces is not always lower than cohesion or internal friction angle of the same soil, but depends on the way by which the interface is formed and roughness of interface. Kulhawy and Peterson (1979) also pointed out that the interface friction angle is less than the soil friction angle for smooth interfaces, and equal to or greater than the soil friction angle for rough interfaces. A rougher interface surface develops when the concrete (or cement grout) is poured directly onto a compacted soil.

To observe the influence of grouting pressure on the interface strength, Hossain and Yin (2014) proposed the following interface shear strength equation for saturated condition considering grouting pressure as an independent parameter:

$$\tau_f = c'_a + \sigma'_{nf} \tan\delta' + p_g \tan\delta^g \quad (2)$$

where, τ_f is the interface shear strength at failure; c'_a is the effective adhesion intercept for gravity grouting (grouting pressure 0 kPa); σ'_{nf} is the effective normal stress variable on the failure plane at failure; δ' is the effective interface friction angle for gravity grouting; p_g is the grouting pressure; and δ^g is the angle indicating the rate of increase in interface shear strength relative to grouting pressure, p_g.

2.2 Unsaturated Condition

Miller and Hamid (2007) modified the shear strength equation for unsaturated soil proposed by Fredlund et al. (1978) to consider for interface between Minco silt and stainless steel. The equation is as follows:

$$\tau_f = c'_a + (\sigma_{nf} - u_{af}) \tan\delta' + (u_a - u_w)_f \tan\delta^b \quad (3)$$

where, τ_f is the interface shear strength at failure; c'_a is the effective adhesion intercept; $(\sigma_{nf} - u_{af})$ is the net normal stress variable on the failure plane at failure; u_{af} is the pore-air pressure at failure; δ' is the effective interface friction angle associated with the net normal stress state variable $(\sigma_{nf} - u_{af})$; $(u_a - u_w)_f$ is the matric suction at failure; and δ^b is the angle indicating the rate of increase in interface shear strength relative to matric suction $(u_a - u_w)_f$.

Sharma et al. (2007) used Bishop's (1959) effective stress equation for unsaturated soil to predict the interface strength of silty sand and geomembrane. The equation is as follows:

$$\tau = \alpha + [(\sigma - u_a) + \chi(u_a - u_w)] \tan\delta \quad (4)$$

where, τ is the interface strength; α is the adhesion; σ is the total normal stress; u_a is the pore-air pressure; u_w is the pore-water pressure; δ is the angle of shearing resistance at the soil-geomembrane interface; and χ is a parameter whose value ranges from 0 to 1. Sharma et al. (2007) pointed out that Eq. (4) does not accurately predict the measured shear strength. At low normal stresses, it overestimates the shear stress relative to the measured values whereas the reverse is true for high normal stresses. Moreover, the resulting χ values ranged from 0.4 to 2.1 for the various series of tests, which is not appropriate.

The shear strength equation for unsaturated soils proposed by Vanapalli et al. (1996) was modified by Hamid and Miller (2009) as follows to predict the shear strength of unsaturated Minco silt-steel interface:

$$\tau_f = c'_a + (\sigma_{nf} - u_{af}) \tan\delta' + (u_{af} - u_{wf}) \tan\delta' \left(\frac{\theta - \theta_r}{\theta_s - \theta_r} \right) \quad (5)$$

where, θ is the current volumetric water content; θ_r is the residual volumetric water content; and θ_s is the saturated volumetric water content obtained from a soil-water retention curve (SWRC).

3. BASIC PROPERTIES OF THE MATERIALS USED

3.1 Completely Decomposed Granite Soil

In this study, completely decomposed granite (CDG) soil, a common soil of the slopes in Hong Kong, was used. This CDG soil was taken from a highway construction site at Tai Wai, Hong Kong. All the tests of the soil followed the procedures as described in (BS 1377: 1990) to determine the basic properties. According to the Unified Soil Classification System (ASTM D2487-90: 1992), the studied CDG soil can be classified as silty sand or SM. The basic properties of the soil are tabulated in Table 1. Figure 1 shows the particle size distribution curve for the studied CDG soil.

Table 1 Basic Properties of the CDG Soil

Property	Unit	Value
Specific gravity	-	2.60
Maximum dry density	mg/m^3	1.75
Optimum moisture content	%	14.3
Void ratio	--	0.485
Gravel	%	5.8
Sand	%	44.1
Silt	%	36.8
Clay	%	13.3
Plastic limit	%	22.7
Liquid limit	%	32.8
Plasticity index	%	10.1
Permeability	m/s	2.36x10^{-8}

3.2 Cement Grout Material

Locally available Portland cement was used to prepare cement grout. The cement was mixed with water at a water/cement ratio of 0.42. The properties of the cement grout material are summarized in Table 2. It should be noted that the properties of the cement grout material were determined at a curing period of 5 days, which was similar to the curing time for the cement grout of the soil-cement interface in the shear box.

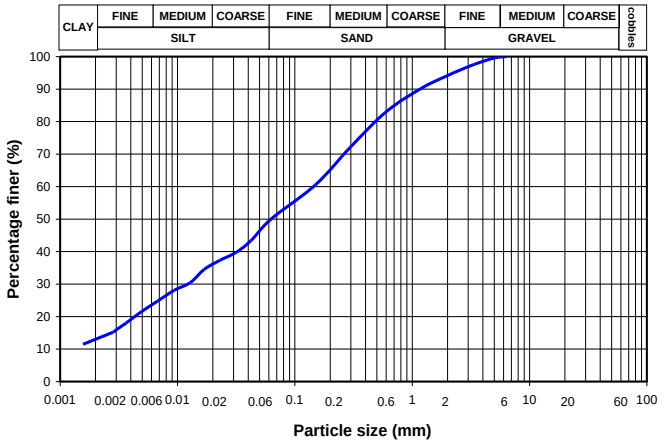

Figure 1 Grain size distribution of the CDG soil

Table 2 Properties of cement grout material

Property	**Unit**	**Value**
Density	mg/m^3	1.89
Uniaxial compressive strength	MPa	32.1
Secant Young's modulus	GPa	12.6
Poisson's ratio	-	0.21

4. PREPARATION OF INTERFACE TEST SPECIMENS

To simulate the cast-insitu installation, cement grout was poured on a compacted surface of the CDG soil. The pretreatment of soil and the procedure of preparing soil-soil direct shear test specimens have been elaborately discussed in Hossain and Yin (2010). The procedure for preparing soil-cement grout specimens under different grouting pressures is described in the following sections.

Before starting the compaction of the CDG soil in the shear box, the two parts of shear box were tightened together by using screws. The gap between the two parts of shear box was filled with grease. The side walls of the shear box were polished with lubricating oil to reduce the friction between soil and side walls. A wooden block (wrapped with scotch tape) having a section of 100 mm by 100 mm and a height of 18 mm was placed at the bottom of the shear box. It should be noted that the height of bottom part of shear box is 20 mm.

The CDG soil was compacted over the wooden block in two layers having a thickness of 10 mm each. Each layer was compacted at optimum moisture content of 14.3% to achieve a controlled dry density of 1.663 mg/m^3, which was 95% of the maximum dry density of 1.75 mg/m^3 obtained using a standard compaction test. The required mass of wet soil for a particular layer was calculated, then placed inside the shear box and compacted. After completing the compaction, the weight of compacted soil was recorded and the top part of the shear box was covered by a steel plate and a wooden block. The gaps between wooden block and side walls of shear box were filled properly with a sealer so that no air can flow through the gaps during pressure grouting. After that the shear box with the compacted soil was turned over (top part down and bottom part up) and placed inside the pressure chamber.

The amount of cement and water needed to fill a section of 100.07 mm by 100.07 mm and a height of 18 mm with cement grout was calculated before mixing. The cement and water were mixed in such a way that no cement particle could coagulate and no lumps could present in the grout. After the preparation of cement grout, the first wooden block was removed to pour cement grout on the prepared surface of soil. The cement grout was poured smoothly over the prepared surface so that the bottom part of shear box could be filled fully with no air voids. Immediately after filling the bottom part of shear box with cement grout, the pressure chamber was closed with the chamber cap, and the preset air pressure (grouting pressure) was applied inside the chamber. The air pressure inside the chamber was maintained for about half an hour (similar to Yin and Zhou, 2009) until the initial setting of the cement grout had almost finished. After that the air pressure valve was closed and pressure was released from the chamber at a very slow rate (approximately 3 kPa per minute) so that no back pressure could be developed which might affect the interface surface. It should be kept in mind that no grouting pressure was applied for normal (gravity) grouting specimen, and cement grout was just placed over the compacted soil surface.

After releasing the pressure, the shear box was moved out from the chamber and kept open in atmosphere for about 12 hours to facilitate the setting of cement grout. After setting, the surface of the cement grout was leveled carefully by using a spatula. The cement grout surface and shear box were wrapped with scotch tape to ensure self-curing of cement grout (to simulate the field condition) for a period of 5 days. After the completion of curing period, the wrapping tape was removed and the shear box was turned over again (soil at top and cement grout at bottom) and set on the shear box base.

5. SELECTION OF INTERFACE LAYER THICKNESS

Hossain and Yin (2012) stated that interface layer thickness may depend on many factors such as way of forming the interface, water-cement ratio of grout, void ratio (porosity) and water content of soil. However, the exact thickness of interface zone for different soil-structure interfaces is still unknown in existing literatures. Considering the findings of previous researches and properties of the studied CDG soil, the authors selected an interface layer thickness of 2 mm for the present testing program, as described in the literature of Hossain and Yin (2012). This means that the soil thickness inside the bottom part of shear box is 2 mm as no gap is provided between the top and bottom parts of shear box.

6. TESTING APPARATUS AND TEST PROCEDURE

For interface direct shear testing, some upgradations were made in the Modified Direct Shear Apparatus (MDSA) used for unsaturated soil direct shear testing. Different from the direct shear testing on an unsaturated soil, the water chamber was constructed inside the top steel platen (similar to Miller and Hamid, 2007) instead of shear box base since the bottom part of specimen was cement grout material as shown in Figure 2. A high air entry ceramic disk was set below the water chamber at the same level of the bottom of top steel platen for testing unsaturated soil-cement grout interface. One end of the water chamber was connected with an auto volume change (AVC) device to measure the flow of water from or into specimen and the other end with a diffused air flushing device (model type: DAF 200M, Geotechnical Consulting & Testing System, LLC) to measure the volume of diffused air. Two LVDTs (Linear Variable Differential Transformer) were used for determining the horizontal and vertical displacement. A load cell, calibrated properly before starting the test program, was used to determine the horizontal shear load. The vertical load was applied by a hanger having a moment arm with dead weights. The specimen and shearing device are enclosed in a pressure chamber, which is made of steel.

Single-stage consolidated drained interface direct shear tests were performed to observe the interface behavior of compacted CDG soil and cement grout under different grouting pressures and matric suctions. The test procedure of conducting interface direct shear test consisted of three steps: saturation, equilibration of matric suction, and drained shearing at constant overburden stress.

6.1 Saturation

The soil-cement grout specimen was placed on the shear box base inside the air pressure chamber, a porous disc plate was placed over the soil, ample amount of water was poured on the disc plate, and the chamber cap was closed. The specimen was allowed to saturate by applying 200 kPa air pressure inside the chamber for about 10 hours. After saturation, the excess water and the disc were removed, the top steel platen fitted with ceramic disc was mounted, the screws used to tighten the top and bottom parts of shear box were released and moved out, and the water chamber was connected with AVC and DAF devices. The height of the specimen was checked before and

after saturation to measure the swelling/contraction. A swelling value of 1.5 mm was found for different specimens after saturation.

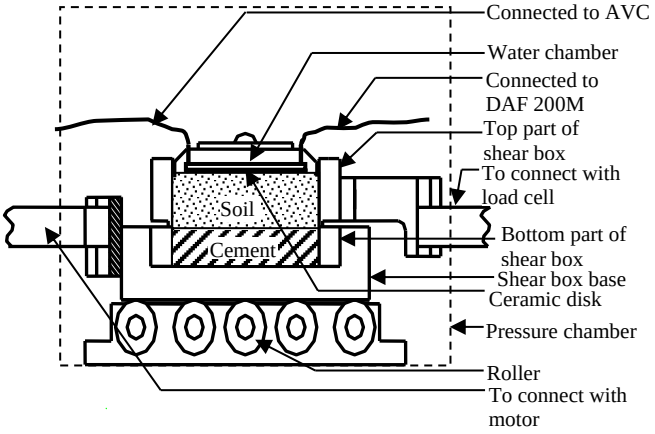

Figure 2 Schematic diagram of MDSA for interface test

6.2 Equilibration of Matric Suction

The pre-calculated axial load, air pressure and water pressure were applied (by opening the valve of AVC) sequentially to attain the desired equilibration of matric suction. The connecting valves of DAF and pressure controller devices remained closed during the equilibration process. It should be noted that axis-translation technique was used to attain the desired matric suction by applying 200 kPa water pressure in the water chamber and the required air pressure in the pressure chamber. Matric suction value is zero for saturated case, and the magnitudes of air pressure and water pressure were equal to 200 kPa. During the equilibration process, vertical deformation and water movement were recorded. Equilibration was assured when the vertical deformation was constant and flow of water essentially ceased.

6.3 Shearing

The specimen was sheared after the equilibration was attained. Single-stage shearing was conducted under a drained condition with a constant shearing rate of 0.004 mm/min (similar to soil-soil direct shear tests) until the horizontal displacement reached at 15 mm. During shearing, the horizontal shear load, horizontal displacement, and vertical displacement were measured and recorded automatically in a computer at an interval of two minutes. Shearing was accomplished during a period of approximately 2.5 days. After the completion of shearing, all the valves were closed, the air pressure was released, and the specimen was quickly dismantled from the shear box for the determination of wet weight of soil.

7. EXPERIMENTAL RESULTS AND DISCUSSION

7.1 Soil-Water Retention Curve (SWRC)

Figure 3 shows the soil-water retention curve (SWRC) for the zero overburden stress by using the modified direct shear apparatus. The degree of saturation decreases as the suction value increases, and the rate of decrement is higher in the suction range of 0 to 100 kPa than the remaining suction range. It is found from Figure 3 that the air entry value of the re-compacted CDG soil is about 11 kPa.

7.2 Soil and Interface Testing at Saturated Condition

Soil-soil direct shear tests and soil-cement grout interface direct shear tests were conducted at saturated condition under different overburden stresses. The soil shear strength and interface shear strength increase with overburden stress. Figure 4 shows the shear strength envelopes for CDG soil and soil-cement interface (gravity grouted) at saturated condition under different overburden stresses. The strength envelopes for both cases are linear. However, the strength envelope for interface is at higher position than that of CDG soil. This may be attributed to the bonding of cement particles with soil in presence of water along the failure plane. The effective angle of internal friction, $\phi' = 29.9°$ and effective cohesion, $c' = 0$ kPa are determined for the compacted CDG soil. Whereas the effective interface friction angle, $\delta' = 31.5°$ and effective adhesion, $c'_a = 16.4$ kPa are obtained for soil-cement interface.

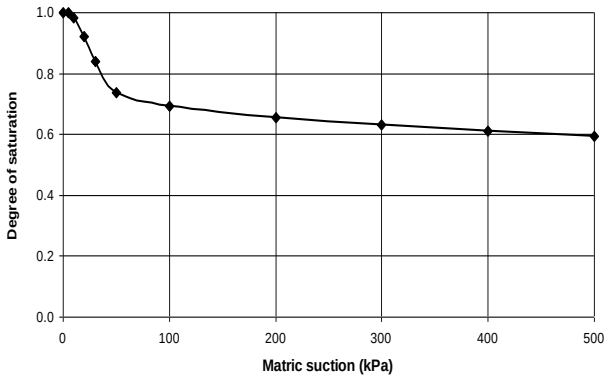

Figure 3 Soil-water retention curve for the CDG soil

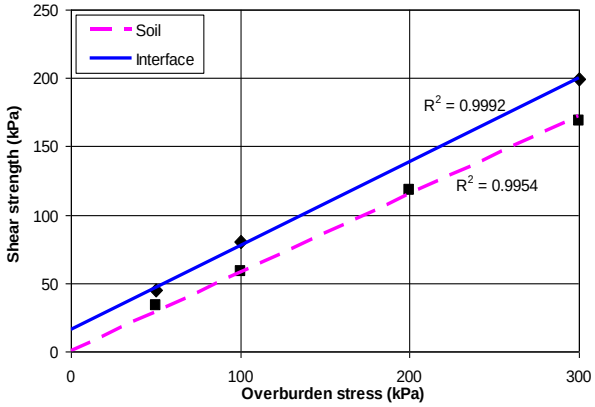

Figure 4 Strength envelopes for CDG soil and gravity grouted soil-cement interface at saturated condition

7.3 Soil and Interface Testing at Unsaturated Condition

7.3.1 Direct Shear Testing on CDG Soil

The stress-displacement relationships of CDG soil for different matric suctions of 0, 50, 100, 200 and 300 kPa under the overburden stress of 50 kPa is presented in Figure 5(a). The stress-strain curves indicate a strain-hardening behavior at lower suctions (0 to 100 kPa). On the contrary, a strain-softening behavior is obvious at higher suctions (100 to 300 kPa). The similar stress-strain behavior is observed under the overburden stresses of 100 and 300 kPa, and the shear stress increases as the overburden stress is increased for the particular matric suction. The deformation behavior of the CDG soil under different suctions and overburden stress of 50 kPa is shown in Figure 5(b). A contractive behavior is observed at saturated condition (0 kPa suction), and the contraction value increases with the increase of overburden stress. However, a dilative behavior is obvious as the suction value is increased from saturated condition. The soil dilation increases with matric suction, and a greater dilation is observed at higher suction under lower overburden stress.

Using the experimental test data, the failure envelopes of the shear stress τ_f at failure with respect to the overburden stress $(\sigma_{nf} - u_{af})$ for different matric suctions $(u_a - u_w)_f$ are shown in Figure 6. It should be noted that area correction for direct shear tests is applied to calculate the shear stress. The failure criterion is considered as the point at which the shear load starts decreasing (peak shear load) or starts to remain fairly constant observed from the raw test data. Figure 6 indicates that the shear strength increases with the overburden stress

and matric suction. The shear strength envelopes of the shear stress τ_f versus the overburden stress $(\sigma_{nf} - u_{af})$ for a given suction are approximately linear. The declivity of those envelopes is presented by apparent friction angle $\phi_{\max}$. The apparent friction angle $\phi_{\max}$ increases with matric suction under different overburden stresses. At saturated condition, $\phi_{\max} = \phi'$. Table 3 presents the values of apparent friction angle $\phi_{\max}$ and cohesion intercept c for different suction values. The cohesion intercept indicates an increase in strength as matric suction increases.

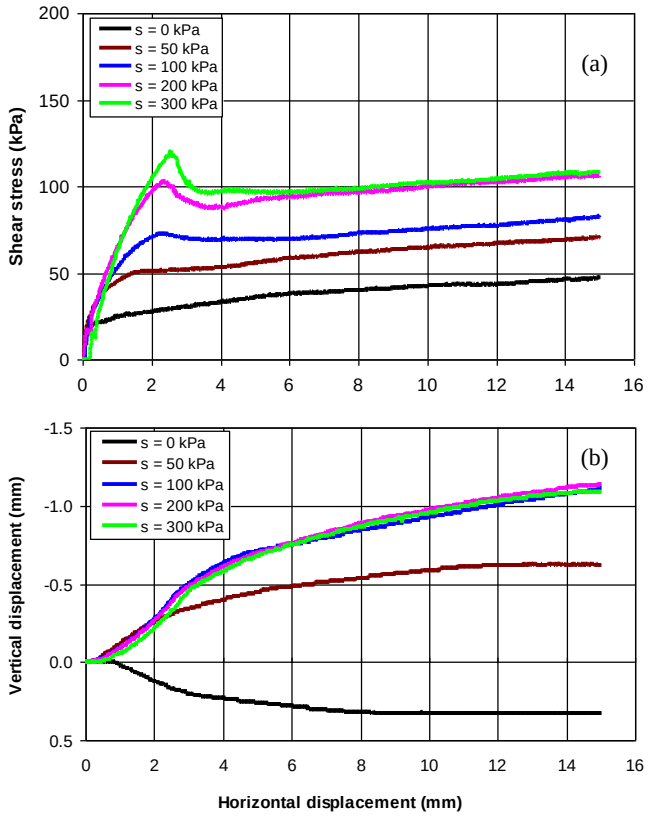

Figure 5 Stress-strain and deformation curves for CDG soil under different suctions and an overburden stress of 50 kPa

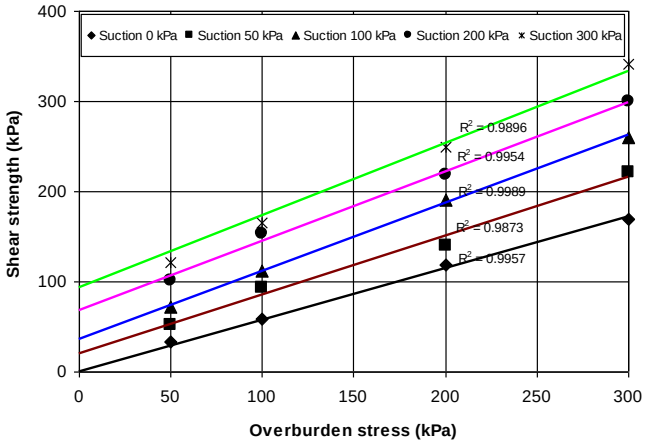

Figure 6 Failure envelopes for the CDG soil corresponding to different suctions

Table 3 Variation of apparent friction angle and cohesion intercept with matric suction for the compacted CDG soil

Matric suction (kPa)	0	50	100	200	300
$\phi_{\max}$ (deg)	29.9	33.1	37.1	37.6	38.7
c (kPa)	0.0	20.6	36.2	68.2	93.5

7.3.2 Direct Shear Testing on Gravity Grouted Interface

The characteristics of gravity grouted soil-cement interface under different matric suctions and an overburden stress of 50 kPa is depicted in Figure 7. The stress-strain characteristics, as described in Figure 7(a), indicates that like the CDG soil interface shear stress increases with the increase of matric suction. A strain-hardening behavior is obvious for saturated condition, and as the suction value is increased a strain-softening behavior is prominent. The similar stress-strain behavior is observed under the overburden stress of 100 and 300 kPa, and the interface shear stress increases with the increase of overburden stress. The deformation behavior of gravity grouted interface, as illustrated in Figure 7(b), indicates a contraction at lower suction, and a dilative behavior is distinct as the suction value is increased. A higher contraction value is observed for higher overburden stress at saturated condition, and a greater dilation is evident under higher suction and lower overburden stress (similar to CDG soil).

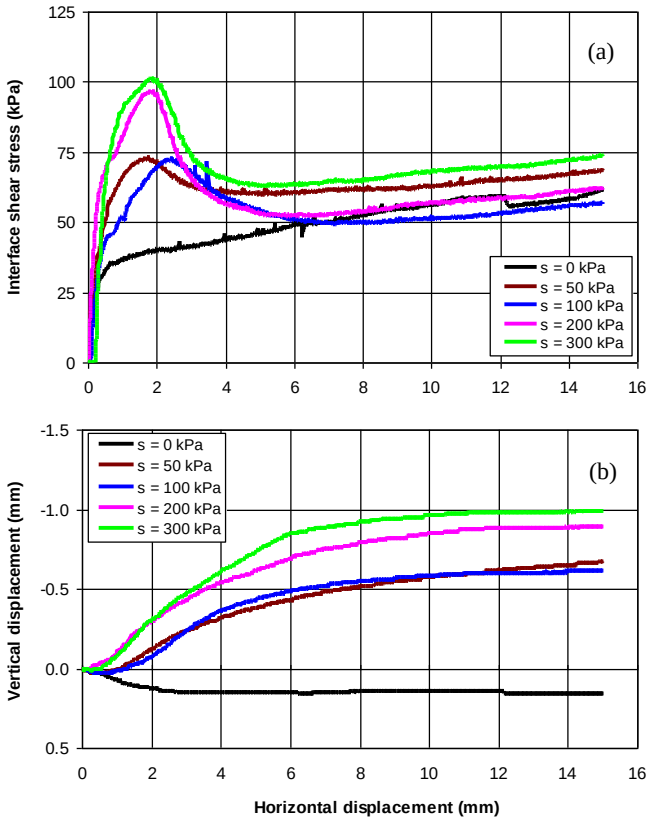

Figure 7 Stress-strain and deformation curves for interface under different matric suctions and an overburden stress of 50 kPa

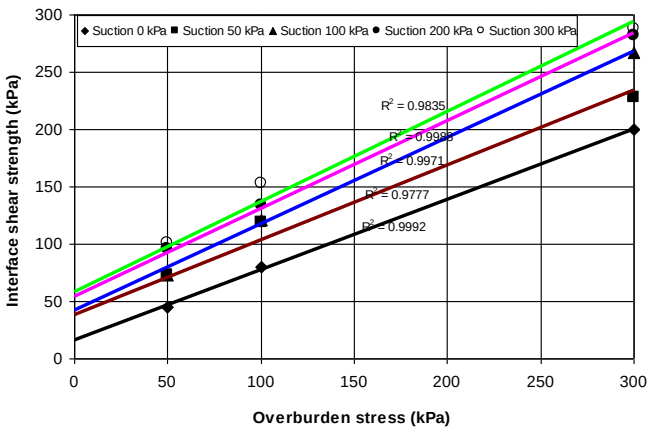

Figure 8 Interface failure envelopes corresponding to different suctions for the gravity grouted soil-cement interface

The relationships between the interface shear strength and the overburden stress (failure envelopes) corresponding to different suctions for gravity grouted soil-cement interface is shown in Figure 8. The interface shear strength envelopes of the shear stress τ_f *versus* the overburden stress $(\sigma_{nf} - u_{af})$ for a given suction are approximately linear. The declivity of those envelopes is represented by apparent interface friction angle $\delta_{\max}$. At saturated condition $\delta_{\max} = \delta'$ and $c_a = c'_a$. The apparent interface friction angle $\delta_{\max}$ and adhesion intercept c_a increase with matric suction. The change of the apparent friction angle is likely attributed to the change of dilation angle with matric suction (Zhan and Ng, 2006; Hossain and Yin, 2010a and b). The change of adhesion intercept is due to change of matric suction and δ^b angle. The values of $\delta_{\max}$ and c_a for different matric suctions are summarized in Table 4.

Table 4 Variation of apparent friction angle and adhesion with matric suction for gravity grouted soil-cement interface

Matric suction (kPa)	0	50	100	200	300
$\delta_{\max}$ (deg)	31.5	33.2	37.0	37.5	38.1
c_a (kPa)	16.4	37.5	41.6	54.0	58.5

7.4 Direct Shear Testing on Pressure Grouted Interface

Figures 9, 10 and 11 show the characteristics of soil-cement grout interface tests under different matric suctions and a overburden stress of 50 kPa for grouting pressures of 80, 130 and 250 kPa, respectively. The relationship of interface shear stress with horizontal displacement for different grouting pressures of 80, 130 and 250 kPa under the matric suctions of 0, 50, 100, 200 and 300 kPa are presented in Figures 9(a), 10(a) and 11(a) for an overburden stress of 50 kPa. Same as the soil-soil direct shear tests and gravity grouted interface tests, the interface shear stress increases with matric suction for different grouting pressures. The interface stress also increases with the increase of overburden stress (100 and 300 kPa). A strain-hardening behavior is observed at saturated condition for different grouting pressures and overburden stresses. However, a strain-softening behavior is obvious when the suction value is increased at lower overburden stresses. Therefore, it can be concluded that grouting pressure, matric suction and overburden stress have interactional significant influence on the interface behavior of soil-cement grout interface.

Figures 9(b), 10(b) and 11(b) describe the variation of vertical displacement with horizontal displacement under the matric suction of 0, 50, 100, 200 and 300 kPa and an overburden stress of 50 kPa for different grouting pressures of 80, 130 and 250 kPa, respectively. Similar to CDG soil and gravity grouted soil-cement interface, a contractive behavior is observed for different grouting pressures at saturated condition. On the other hand, a dilative behavior is prominent as the suction value is increased from saturated condition. The similar behavior is observed under the overburden stresses of 100 and 300 kPa. However, the dilation values of soil-cement interface for different grouting pressures are lower compared to that of CDG soil. This indicates that in case of interface tests at unsaturated condition, soil particles may move around each other during shearing due to infiltration of cement particles along the failure surface. Also, the contraction values of interface tests at saturated condition for different grouting pressures are lower than that of CDG soil. This may be due to the fact that soil particles along the failure surface may be locked in place by cement bonds, which resist the vertical deformation during shearing.

The failure envelopes for different matric suctions corresponding to different grouting pressures of 80, 130 and 250 kPa are shown in Figures 12(a), 12(b) and 12(c), respectively. The shear strength is obtained from the raw test data according to the criteria used in case of CDG soil. The interface shear strength envelopes for different matric suctions corresponding to different grouting pressures are approximately linear. The declivity of those envelopes is represented by apparent interface friction angle $\delta_{\max}$. At saturated condition, $\delta_{\max} = \delta'$. The values of apparent interface friction angle $\delta_{\max}$ and apparent adhesion intercept $c'_{a(g)}$ obtained from failure envelopes are tabulated in Table 5. Similar to CDG soil, the apparent interface friction angle $\delta_{\max}$ increases with matric suction for particular grouting pressure. On the contrary, it decreases with pressure grouting for different matric suctions except saturated condition. The decrease of apparent interface friction angle with pressure grouting may be attributed to the decrease of interface dilation angle. The interface dilation angle may be decreased due to slippage of the interface soil particles as the cement particles infiltrates into the failure plane. The more the grouting pressure, the more the infiltration of cement particles. The apparent adhesion intercept for different grouting pressures $c_{a(g)}$ increases with matric suction and grouting pressure. The increase of adhesion intercept at saturated condition (0 kPa suction) is attributed to the bonding of soil particles with hydrated cement particles. The change of adhesion intercept at unsaturated condition is due to change of matric suction and δ^b angle. The adhesion intercept $c_{a(g)}$ can be defined by the following equation considering the influence of matric suction and grouting pressure:

$$c_{a(g)} = c'_a + p_g \tan\delta^g + (u_a - u_w)_f \tan\delta^b \quad (6)$$

where, c'_a is the effective adhesion; p_g is the grouting pressure; δ^g is the angle indicating the rate of increase of interface shear strength relative to grouting pressure p_g; $(u_a - u_w)_f$ is the matric suction at failure; and δ^b is the angle indicating the rate of increase in interface shear strength relative to matric suction $(u_a - u_w)_f$.

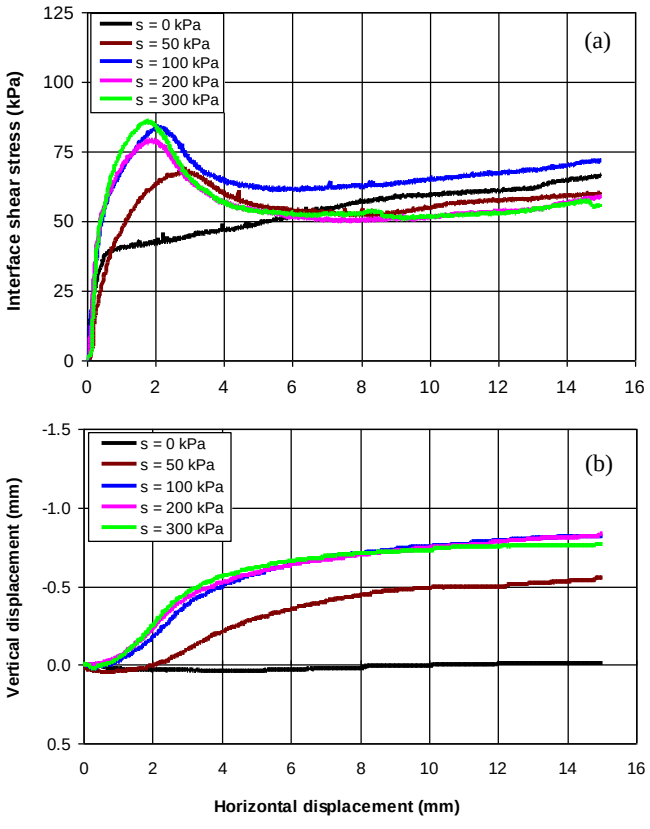

Figure 9 Stress-strain and deformation curves for pressure grouted interface (GP 80 kPa) under an overburden stress of 50 kPa

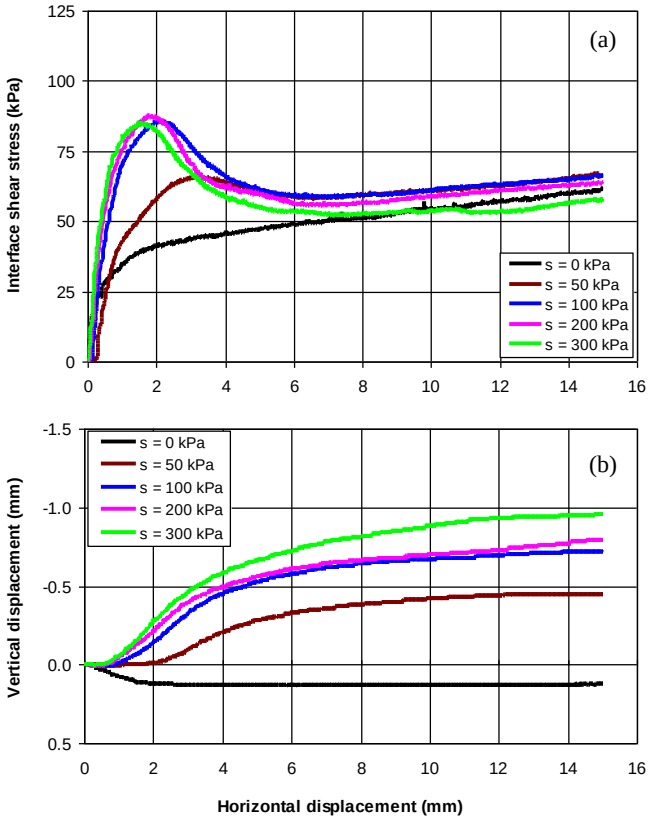

Figure 10 Stress-strain and deformation curves for pressure grouted interface (GP 130 kPa) under an overburden stress of 50 kPa

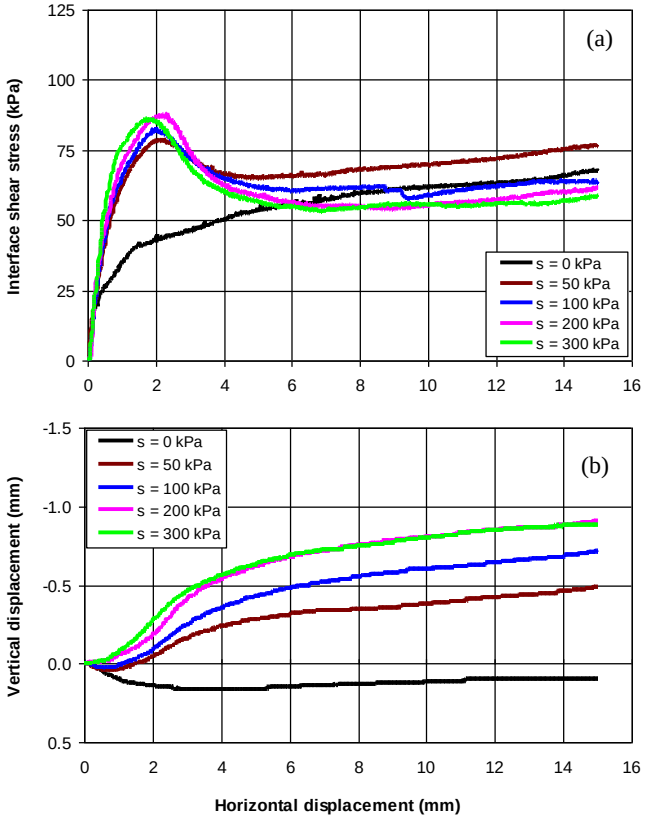

Figure 11 Stress-strain and deformation curves for pressure grouted interface (GP 250 kPa) under an overburden stress of 50 kPa

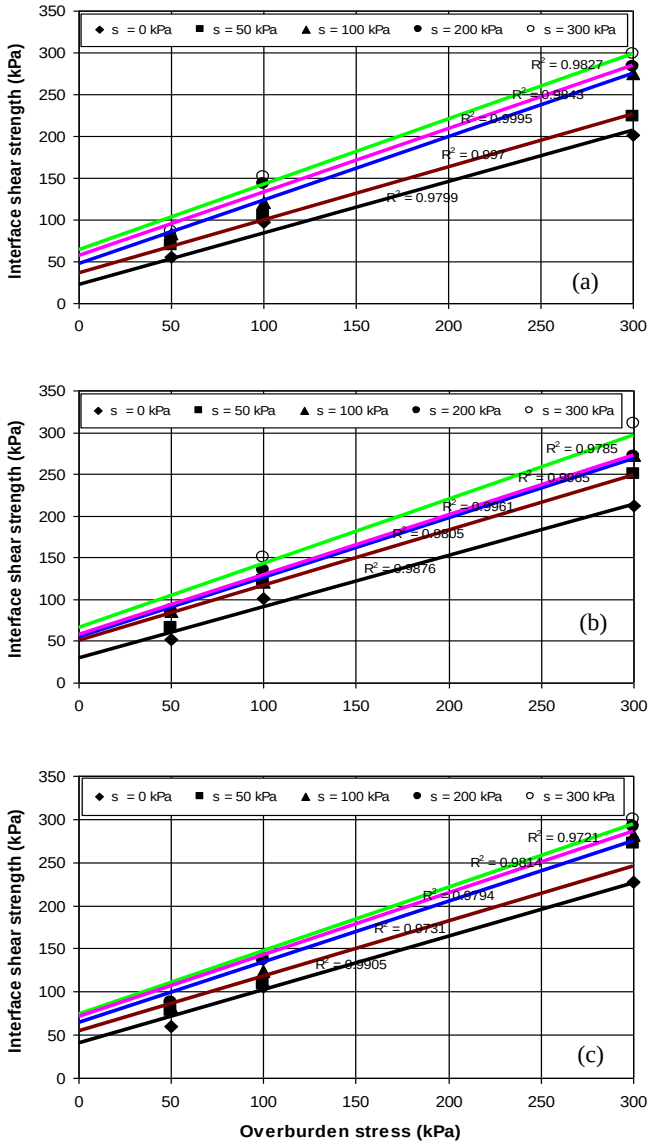

Figure 12 Interface failure envelopes for grouting pressure: (a) 80 kPa, (b) 130 kPa, and (c) 250 kPa

Table 5 Variation of apparent interface friction angle and adhesion intercept with matric suction and grouting pressure

Grouting pressure (kPa)		Matric suction (kPa)				
		0	**50**	**100**	**200**	**300**
0	δ_{max} (deg)	31.5	33.2	37.0	37.5	38.1
	$c_{a(g)}$ (kPa)	16.4	37.5	41.6	54.0	58.5
80	δ_{max} (deg)	31.5	32.4	37.0	37.3	38.0
	$c_{a(g)}$ (kPa)	22.5	36.2	47.7	56.4	64.5
130	δ_{max} (deg)	31.5	33.2	35.5	35.6	37.5
	$c_{a(g)}$ (kPa)	30.5	51.3	55.5	57.4	65.8
250	δ_{max} (deg)	31.5	32.5	35.0	35.6	36.2
	$c_{a(g)}$ (kPa)	41.8	54.7	64.7	70.9	73.9

8. CONCLUSIONS

The direct shear test results of compacted CDG soil-cement grout interface and their interpretations for different suctions, grouting pressures and overburden stresses are presented in the present paper. The interface behavior is compared with the behavior of the same CDG soil. The following conclusions are drawn based on the discussion depicted in the previous sections:

(a) The soil-cement interface shear strength increases with overburden stress. At saturated condition, the stress-strain behavior shows strain-hardening, and the deformation behavior indicates contraction for both CDG soil and interface.
(b) The failure envelopes for both CDG soil and interface are quite linear. The relative position of failure envelopes indicates that the soil-cement interface strength is greater than that of compacted CDG soil at saturated condition.
(c) The interface shear stress increases with matric suction for different grouting pressures and overburden stresses, and a strain-softening behavior is obvious when the suction value is increased from saturated condition for different overburden stresses. However, for CDG soil, a strain-softening behavior is observed only at higher suction range.
(d) A dilative behavior is obvious for interface as the suction value is increased from saturated condition under individual overburden stresses. However, the dilation values of soil-cement interface for different grouting pressures are smaller compared to CDG soil under different suctions and overburden stresses.
(e) The interface shear strength envelopes for different matric suctions corresponding to different grouting pressures are approximately linear. Similar to CDG soil, the apparent interface friction angle increases with matric suction for particular grouting pressure. On the contrary, it decreases with pressure grouting for different matric suctions except saturated condition. The apparent adhesion intercept for different grouting pressures increases with matric suction and grouting pressure.

9. ACKNOWLEDGEMENTS

The work in this paper is supported by a National State Key Project “973” grant (Grant No.: 2014CB047000) (sub-project No. 2014CB047001) from Ministry of Science and Technology of the People’s Republic of China, a CRF project (Grant No.: PolyU12/CRF/13E) from Research Grants Council (RGC) of Hong Kong Special Administrative Region Government of China. The authors acknowledge also the financial supports from Research Institute for Sustainable Urban Development of The Hong Kong Polytechnic University.

10. REFERENCES

American Society for Testing and Materials (1992) ASTM D2487-90: 1992. Standard test method for classification of soils for engineering purposes (Unified Soil Classification System), Annual Books of ASTM Standards, Vol. 04.08, Section 4, Philadelphia, Penn: 326-336

Berglund, C., and Oden, K. (1996) "The pullout resistance of different types of nails", MS thesis, Dept. of Geotechnical Engineering, Chalmers Univ. of Technology, Göteborg, Sweden.

Bishop, A. W. (1959) "The principle of effective stress", Lecture delivered in Oslo, Norway, in 1955, Tecknisk Ukeblad I Samarbeide Med Teknikk, 106, issue 39, pp859-863.

British Standards Institution. (1990) British Standard BS 1377: 1990, Methods of test for soils for civil engineering purposes, London, UK

Burland, J. B., and Ridley, A. K. (1996) "The importance of suction in soil mechanics", 12th Geotechnical Southeast Asian Conference, Kuala Lumpur, issue 2, pp27–49.

Chu, L. M., and Yin, J. H. (2005) "Comparison of interface shear strength of soil nails measured by both direct shear box tests and pullout tests", Journal of Geotechnical and Geoenvironmental Engineering, ASCE, 131, issue 9, pp1097-1107.

Franzen, G. (1998) "Soil nailing- A laboratory and field study of pullout capacity", PhD thesis, Chalmers Univ. of Technology, Chalmers, Sweden.

Fredlund, D. G., Morgenstern, N. R., and Widger, R. A. (1978) "The shear strength of unsaturated soils", Canadian Geotechnical Journal, 15, issue 3, pp313-321.

Fredlund, D. G., and Rahardjo, H. (1993) "Soil mechanics for unsaturated soils”, John Wiley and Sons, Inc., New York.

Hamid, T. B., and Miller, G. A. (2009) "Shear strength of unsaturated soil interfaces", Canadian Geotechnical Journal, 46, pp595-606.

Heymann, G. (1993) "Soil nailing systems as lateral support for surface excavations", MS thesis, Faculty of Engineering, Univ. of Pretoria, Pretoria, South Africa.

Hossain, M. A., and Yin, J. H. (2014) "Behavior of a pressure grouted soil-cement interface in direct shear tests", International Journal of Geomechanics, ASCE, 14, issue 1, pp101-109.

Hossain, M. A., and Yin, J. H. (2012) "Influence of grouting pressure on the behavior of an unsaturated soil-cement interface", Journal of Geotechnical and Geoenvironmental Engineering, ASCE, 138, issue 2, pp193-202.

Hossain, M. A., and Yin, J. H. (2010a) "Behavior of a compacted completely decomposed granite soil from suction controlled direct shear tests", Journal of Geotechnical and Geoenvironmental Engineering, ASCE, 136, issue 1, pp189-198.

Hossain, M. A., and Yin, J. H. (2010b) "Shear strength and dilative characteristics of an unsaturated compacted completely decomposed granite soil", Canadian Geotechnical Journal,47, pp1112-1126.

Kulhawy, F. H., and Peterson, M. S. (1979) "Behavior of sand-concrete interfaces", Proceedings of the 6th Pan-American Conference on Soil mechanics and Foundation Engineering, Vol. 7, International Society for Soil Mechanics and Geotechnical Engineering, London, pp225-236

Lee, C. F., Law, K. T., Tham, L. G., Yue, Z. Q., and Junaideen, S. M. (2001) "Design of a large soil box for studying soil-nail interaction in loose fill", Soft soil engineering, pp413-418.

Miller, G. A., and Hamid, T. B. (2007) "Interface direct shear testing of unsaturated soil", Geotechnical Testing Journal, 30, issue 3, pp1-10.

Potyondy, J. G. (1961) "Skin friction between various soils and construction materials”, Géotechnique, 11, issue 4, pp339-353.

Pun, W. K., and Shiu, Y. K. (2007) "Design practice and technical developments of soil nailing in Hong Kong", Proceedings of HKIE Geotechnical Division, 27th Annual Seminar: Geotechnical Advancements in Hong Kong since 1970s, Hong Kong, pp197-212.

Sharma, J. S., Fleming, I. R., and Jogi, M. B. (2007) "Measurement of unsaturated soil-geomembrane interface shear-strength parameters", Canadian Geotechnical Journal, 44, pp78-88.

Vanapalli, S. K., Fredlund, D. G., Pufahl, D. E., and Clifton, A. W. (1996) "Model for the prediction of shear strength with respect to soil suction", Canadian Geotechnical Journal, 33, pp379-392.

Yeung, A. T., Cheng, Y. M., Lau, C. K., Mak, L. M., Yu, R. S. M., Choi, Y. K., and Kim, J. H. (2005) "An innovative Korean system of pressure grouted soil nailing as a slope stabilization measure", Proceedings of HKIE Geotechnical Division, 25thAnnual Seminar, 4 May, Hong Kong, Published by HKIE-GDC and HKGES, pp43-49.

Yin, J. H., Su, L. J., Cheung, R. W. M., Shiu, Y. K., and Tang, C. (2008) "The influence of grouting pressure on the pullout resistance of soil nail in compacted completely decomposed granite fill", Géotechnique, 59, issue2, pp103-113.

Yin, J. H., and Zhou, W. H. (2009) "Influence of grouting pressure and overburden stress on the interface resistance of a soil nail", Journal of Geotechnical and Geoenvironmental Engineering, ASCE, 135, issue 9, pp1198-1208.

Zhan, T. L. T., and Ng, C. W. W. (2006) "Shear strength characteristics of an unsaturated expansive clay", Canadian Geotechnical Journal, 43, issue 8, pp751-763.